

**EVOLUTION OF A VAPOR CAVITY DURING
EXPLOSIVE BOILING ON A FILM MICROHEATER:
EXPERIMENT AND NUMERICAL SIMULATION**

**Yu. D. Varlamov,¹ Yu. P. Meshcheryakov,² S. I. Lezhnin,¹
M. R. Predtechenskii,¹ and S. N. Ul'yankin¹**

UDC 536.423

Dynamics of formation, growth, and collapse of a vapor cavity during explosive boiling of liquids on film heaters under the action of pulsed heat fluxes $q = 10^8$ – 10^9 W/m² is studied theoretically and experimentally. The description of the vapor-cavity formation process is based on the concept of a homogeneous mechanism of nucleation taking into account the influence of already formed and growing bubbles. Evolution of vapor structures is numerically simulated by solving the equations of dynamics of a compressible liquid with allowance for heat transfer, evaporation, and condensation. A comparison of experimental and numerical data shows that the model proposed offers an adequate description of the main features of explosive boiling of liquids on film heaters, including the effect of conditions of the thermal action and liquid properties on the duration of cavity evolution and on the cavity size.

Key words: *explosive boiling, formation and evolution of a vapor cavity, numerical simulation.*

Introduction. High growth rates of temperature in liquids (above 10^6 K/sec) near the surface of low-inertia heaters lead to significant overheatings to a level of spontaneous nucleation of vapor bubbles, and explosive boiling occurs [1–4] with formation of a thin vapor cavity due to coalescence of rapidly growing microbubbles and subsequent growth and collapse of the cavity. This phenomenon is widely used in various micromechanical devices, including jet printers [5], microactuators [6], and micropumps [7]; hence, optimization of operation conditions of these devices requires understanding of the explosive boiling process.

Overheating of liquids and fluctuation nucleation as a dominating mechanism determining the beginning of explosive boiling have been studied in many papers (see, e.g., [1–5, 8–11]). The further evolution of the process is less known [5, 7, 12, 13]. In particular, the stage of generation, growth, and coalescence of microbubbles has not been adequately addressed, whereas the vapor pressure and the volume of the cavity formed at this stage, as well as the distribution of temperatures in the liquid around the cavity are largely responsible for the subsequent evolution of the cavity.

To describe the evolution of the vapor cavity, Asai [5] proposed using an empirical equation with an exponentially decaying dependence of the vapor pressure in the cavity on time. The initial pressure was assumed to be the pressure of saturated vapors corresponding to the conditions of boiling incipience. It is known, however, that the initial size of bubbles in the case of homogeneous nucleation stays in the nanometer range [1, 2, 9]. Before their coalescence in the cavity, the bubbles can reach a micrometer-scale size [1, 10, 11], i.e., their radius increases by more than two orders of magnitude. A significant change in pressure in the bubbles in the course of their growth can

¹Kutateladze Institute of Thermophysics, Siberian Division, Russian Academy of Sciences, Novosibirsk 630090; varlamov@itp.nsc.ru. ²Design and Technology Department of the Lavrent'ev Institute of Hydrodynamics, Siberian Division, Russian Academy of Sciences, Novosibirsk 630090. Translated from *Prikladnaya Mekhanika i Tekhnicheskaya Fizika*, Vol. 48, No. 4, pp. 79–87, July–August, 2007. Original article submitted April 5, 2006; revision submitted June 7, 2006.

be expected. As a result, the initial pressure in the cavity formed owing to bubble coalescence differs substantially from the pressure of saturated vapors corresponding to the temperature of boiling incipience. The further evolution of the vapor cavity also depends on the temperature distribution in the liquid and on the liquid properties. Hence, to describe this process, one has to consider jointly the problem of dynamics of the liquid with free surfaces and the problem of conjugate heat transfer accompanied by nonequilibrium processes of evaporation and condensation on the interface.

Solving this problem in the present work involved numerical simulations of the dynamics of formation, growth, and collapse of the vapor cavity. The description of homogeneous incipience under conditions of substantial overheating of the liquid is based on the fluctuation mechanism of nucleation; the influence of already formed and growing bubbles was also taken into account. In numerical simulations of the evolution of vapor structures, we used the solution of the equations of dynamics of a compressible liquid with allowance for heat transfer, evaporation, and condensation. The results of numerical simulations were compared with experimental data (conditions provoking explosive boiling of the liquids, time scales of the process, and character of changes in the vapor-cavity shape in the course of its evolution).

1. Test Techniques. In experiments on explosive boiling of liquids under the action of pulsed heat fluxes, we used the technique of stroboscopic visualization of the stages of fast processes (with a time resolution of 100 nsec) with subsequent reconstruction of the sequence of these stages [14]. The liquids were heated on a $100 \times 100 \mu\text{m}$ film heater whose multilayered structure was described in [12]. The tested liquids were water, toluene, ethanol, and isopropyl alcohol. Explosive boiling in the present experiments was initiated by heat fluxes $q = 10^8\text{--}10^9 \text{ W/m}^2$; the heat-pulse duration was $\tau_h = 2\text{--}10 \mu\text{sec}$. To compare the results with numerical simulations, we determined the time of the beginning of various stages of boiling and the changes in the shape and geometric size of the vapor structures in the course of their evolution.

2. Model of the Explosive Boiling Process. Three stages can be conventionally classified in the development of explosive boiling caused by pulsed heating: 1) heating of the film heater and liquid before boiling incipience; 2) spontaneous origination of vapor bubbles, their growth, and coalescence into a vapor cavity; 3) cavity growth and collapse.

2.1. *Beginning of Explosive Boiling.* The modeling of the stage of heating of the film heater and liquid prior to origination of a single bubble was based on the numerical solution of two-dimensional equations of heat conduction in each layer of the film structure of the heater and in the liquid layer contacting the heater. A detailed description of the model can be found in [14]. The parameters to be calculated were the distribution of the liquid temperature near the heater surface and its variation in time $T(t)$. The beginning of liquid boiling was assumed to be the time $t = \tau_b$ when the temperature of the liquid near the heater reached $T = T_b$ at which one bubble was formed on the heater surface of area S . This condition can be written as the equation [14]

$$S \int_0^{\tau_b} J(T(t)) dt = 1, \quad (1)$$

where J is the rate of nucleation (number of nuclei formed per unit time on a unit surface of the heater). Based on the data obtained in [14] and on the results of [1, 5, 9–13], we assumed that spontaneous nucleation is the dominating mechanism of explosive boiling incipience at heat fluxes $q > 10^8 \text{ W/m}^2$ and determined the nucleation rate J (see [14]) in accordance with the theory of homogeneous nucleation [8, 9]. The calculated times and temperatures of boiling incipience and the temperature distribution near the heater surface were the initial conditions in numerical simulations for the next stage of boiling.

2.2. *Model of Spontaneous Nucleation of Vapor Bubbles, Their Growth, and Coalescence into a Cavity.* Coalescence of newly generated and already growing bubbles results in formation of a vapor film that covers the entire surface of the heater. Taking into account that the existing and growing bubbles cover part of the heater surface, thus, decreasing the probability of nucleation of new bubbles [4], we determined the rate of bubble generation by the equation

$$\frac{dN}{dt} = SJ(T(t))[1 - \varphi(t)], \quad (2)$$

where the parameter

$$\varphi(t) = \frac{1}{S} \int_0^t \frac{dN}{d\tau} \pi [R(t-\tau)]^2 d\tau \quad (3)$$

characterizes the fraction of the heater surface covered by bubbles at the time t , i.e., the surface concentration of bubbles. In Eq. (3), $R(t)$ is the radius of a single bubble as a function of time and N is the number of bubbles.

The theory of homogeneous nucleation [8, 9] implies that the external pressure and the liquid temperature are the governing parameters determining the nucleation rate J . In the course of generation of the bubbles and their coalescence into a cavity, the pressure in the liquid near the heater changes from the atmospheric value P_a (when the number of bubbles is small) to the mean value of the vapor pressure in the bubbles P_s at the moment of their coalescence $t = \tau_c$. The heat flux from the heater to the liquid (and, hence, the growth rate of the liquid temperature) changes from the value corresponding to the heat flux at boiling incipience $t = \tau_b$ to a low value (heat flux into the vapor layer) corresponding to the moment of bubble coalescence and formation of the vapor cavity $t = \tau_c$. Thus, the range of pressures and temperature growth rates during cavity formation being found, we can use the linear dependence of these parameters on the surface concentration of bubbles $\varphi(t)$ as the next approximation [see Eq. (3)]:

$$P(t) = P_a + (P_s(\tau_c) - P_a)\varphi(t), \quad (4)$$

$$\frac{dT}{dt}(t) = \left(\frac{dT}{dt}\right)_b (1 - \varphi(t)), \quad T(t) = T_b + \int_{\tau_b}^t \frac{dT}{d\tau}(\tau) d\tau.$$

Here $P(t)$ is the pressure in the liquid and $(dT/dt)_b$ is the growth rate of the liquid temperature at boiling incipience.

The dependence $R(t)$ in Eq. (3) was determined through the numerical solution of the problem of growth of a single bubble in a nonuniformly heated liquid. We solved the Euler equations of the dynamics of an ideal compressible liquid together with the heat-conduction equation within the framework of spherical symmetry [15]:

$$\frac{\partial \rho r^2}{\partial t} + \frac{\partial \rho u r^2}{\partial r} = 0, \quad \frac{\partial (\rho c_p T)}{\partial t} + u \frac{\partial (\rho c_p T)}{\partial r} = \frac{1}{r^2} \frac{\partial}{\partial r} \left(r^2 \lambda \frac{\partial T}{\partial r} \right), \quad (5)$$

$$\frac{\partial \rho u r^2}{\partial t} + \frac{\partial (\rho u^2 + P) r^2}{\partial r} = 2rP, \quad \frac{\partial \rho (e + u^2/2) r^2}{\partial t} + \frac{\partial [\rho u (e + u^2/2) + Pu] r^2}{\partial r} = 0.$$

Here ρ is the density, c_p is the specific heat, λ is the thermal conductivity, e is the specific internal energy, P is the pressure, and u is the radial component of the velocity vector. The system was closed by the equations of state $P = (\gamma - 1)\rho e + C_0^2(\rho - \rho_0)$ for the liquid and $P = (\gamma - 1)\rho e$ for the vapor, where γ is the ratio of specific heats, ρ_0 is the initial density, and C_0 is the velocity of sound. The internal energy of the vapor was found by the formula $e = c_p T$.

The principle of local thermodynamic equilibrium was used on the vapor–liquid interface. The vapor and liquid temperatures on the interface were assumed to be equal to the saturation temperature for this pressure $T_s(P)$. The vapor pressure and temperatures were assumed to be spatially homogeneous. This assumption was valid because the characteristic size of the vapor structures R is small and the thermal wave obeys the condition $(a_v \tau_v)^{1/2} > R$, where a_v is the thermal diffusivity of the vapor and τ_v is the characteristic time of existence of the vapor structure.

The interface velocity was assumed to be equal to the velocity of the liquid on the interface. The change in the vapor mass (due to evaporation and condensation) was determined by the specific mass flux on the interface

$$j = \frac{1}{L} \left(\lambda_l \frac{\partial T_l}{\partial n} - \lambda_v \frac{\partial T_v}{\partial n} \right), \quad (6)$$

where n is the normal to the interface, L is the latent heat of evaporation, and T_l , T_v , λ_l , and λ_v are the temperatures and thermal conductivities of the liquid and vapor, respectively.

The initial pressure of the vapor in the bubble was assumed to be equal to the saturation pressure P_s at the temperature of the beginning of bubble formation T_b . The initial bubble radius R_0 is determined from the condition of its nucleation

$$P_s(T_b) - P_a = 2\sigma(T_b)/R_0,$$

where σ is the surface tension of the liquid.

The heated layer of the liquid being assumed to be displaced without mixing during the growth of the vapor nucleus, the initial distribution of temperature in the liquid around the bubble was assumed to be the temperature distribution near the heater surface at the moment of formation of the vapor nucleus. On the outer boundary of the liquid layer, the condition of zero heat fluxes was used, and the pressure was assumed to be equal to the ambient pressure P_a .

The solution of the problem on growth of a single bubble made it possible to determine the pressure, density, and temperature of the vapor in the bubbles in the course of their growth and at the moment of their coalescence and cavity formation. The moment of cavity formation $t = \tau_c$ was assumed to be the time when the condition $dN/dt = 0$ holds, i.e., in accordance with Eq. (3), when the total area occupied by the bubbles becomes equal to the heater area S [or $\varphi(\tau_c) = 1$].

The total volume of the bubbles (the volume of the cavity V_c) at the moment of their coalescence $t = \tau_c$ was determined by the formula

$$V_c = \int_0^{\tau_c} \frac{dN}{d\tau} \frac{2\pi}{3} [R(t - \tau)]^3 d\tau. \quad (7)$$

After that, with allowance for the total internal energy of the vapor as an ideal gas, we found the mean pressure in the cavity

$$P_c = \int_0^{\tau_c} \frac{dN}{dt} \frac{2\pi}{3} [R(\tau_c - t)]^3 P(\tau_c - t) dt / \int_0^{\tau_c} \frac{dN}{dt} \frac{2\pi}{3} [R(\tau_c - t)]^3 dt. \quad (8)$$

The system of integrodifferential equations (2)–(8) was solved by an iterative method. The parameters calculated for a prescribed heat flux were the time of formation of the vapor cavity τ_c , the cavity volume V_c , the pressure P_c , the temperature T_c , and the density of the vapor in the cavity, i.e., the initial conditions governing the subsequent process of evolution of the vapor cavity.

2.3. Model of Growth and Collapse of the Vapor Cavity. As in the case of modeling of single bubble growth, we described the cavity growth and collapse by the Euler equations of the dynamics of an ideal compressible liquid, jointly with the heat-conduction equation [15]. The initial shape of the vapor cavity was modeled by a thin disk, and the problem of describing its further evolution was solved in the approximation of cylindrical symmetry:

$$\begin{aligned} \frac{\partial \rho r}{\partial t} + \frac{\partial \rho u r}{\partial z} + \frac{\partial \rho v r}{\partial r} &= 0, \\ \frac{\partial \rho u r}{\partial t} + \frac{\partial (\rho u^2 + P)r}{\partial z} + \frac{\partial \rho u v r}{\partial r} &= 0, \quad \frac{\partial \rho v r}{\partial t} + \frac{\partial \rho u v r}{\partial z} + \frac{\partial (\rho v^2 + P)r}{\partial r} = P, \\ \frac{\partial \rho (e + |u|^2/2)r}{\partial t} + \frac{\partial [\rho u (e + |u|^2/2) + P u]r}{\partial z} + \frac{\partial [\rho v (e + |u|^2/2) + P v]r}{\partial r} &= 0, \\ \frac{\partial (\rho c_p T)}{\partial t} + u \frac{\partial (\rho c_p T)}{\partial z} + v \frac{\partial (\rho c_p T)}{\partial r} &= \frac{1}{r} \frac{\partial}{\partial z} \left(r \lambda \frac{\partial T}{\partial z} \right) + \frac{1}{r} \frac{\partial}{\partial r} \left(r \lambda \frac{\partial T}{\partial r} \right) \end{aligned} \quad (9)$$

($|u|$ is the absolute value of the velocity vector).

The specific mass flux on the interface was determined by Eq. (6). The conditions of identical temperatures and fluxes and the zero normal component of velocity were set on the cavity–heater interface. The motion of a point on the liquid–gas–solid contact line was calculated by the algorithm described in [15], where the normal component of velocity on this line equals zero, like for all points on the solid surface, while the tangential component is determined by the projection of the velocity vector of the interface in a small vicinity of the solid surface onto this surface. The remaining conditions and assumptions on the vapor temperature on the interface, spatial homogeneity of vapor pressure and temperature, and interface velocity are the same as those used in Section 2.2 in the model of growth of a single bubble.

The initial geometric size and thermodynamic parameters of the vapor cavity were obtained by solving the problem formulated in Section 2.2 [see Eqs. (2)–(8)]. The initial temperature distribution in the liquid around the

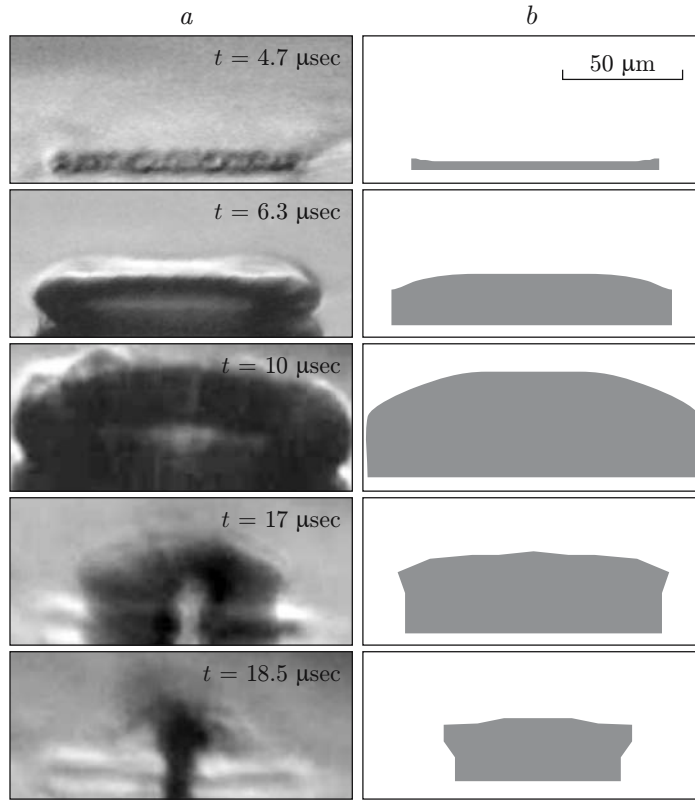


Fig. 1. Changes in the shape of the vapor cavity in the course of its evolution in the case of ethanol boiling ($q = 3.1 \cdot 10^8 \text{ W/m}^2$ and $\tau_h = 4.4 \mu\text{sec}$): experimental data (a) and numerical simulations (b).

cavity was assumed to be similar to the temperature distribution around individual bubbles at the moment of their coalescence into a cavity. The initial momentum imparted, in the course of bubble growth, to the liquid layer near the cavity in the normal direction was described by the following formula in the linear approximation:

$$p_0 = (P(\tau_b) + P(\tau_c))(\tau_c - \tau_b)S_c n.$$

Here S_c is the area of the cavity surface bordering with the liquid, $P(\tau_b)$ is the vapor pressure in the bubbles at the moment of their nucleation, and $P(\tau_c)$ is the vapor pressure in the bubbles at the moment of their coalescence into a vapor cavity.

3. Brief Description of Numerical Procedures and Algorithms. The Euler equations (6) and (10) were numerically solved on the basis of an explicit conservative monotonic scheme of the type of the Riemann problem, with the first order of accuracy $O(\tau + h)$, on moving grids depending on the gradients of the solution [15]. The laws of conservation of mass, momentum, and energy were satisfied exactly. The numerical solution of the heat-conduction equation was based on using an implicit conservative scheme of the second order of accuracy $O(\tau + h^2)$, where the heat balance was also satisfied exactly. The system of linear equations obtained by approximation was solved by a sweep method. Numerical integration was performed by a method of trapezoids.

4. Comparison of Numerical Simulations and Experimental Data. The results of simulating the stage of heating of the film heater and liquid prior to boiling were described in [14]. It was also shown there that the results of numerical simulations agree with experimentally obtained values of temperature and times of boiling incipience of the examined liquids at heat fluxes $q = 10^8\text{--}10^9 \text{ W/m}^2$.

The change in the cavity shape from the moment of its formation to collapse in the course of ethanol boiling is illustrated in Fig. 1. Figure 2 shows the time evolution of the height of the central part of the cavity H and the radial size of the cavity D . It is seen that the results of numerical simulations agree with experimental data. An apparent reason for the differences observed at the stage of the cavity collapse is the use of an approximation

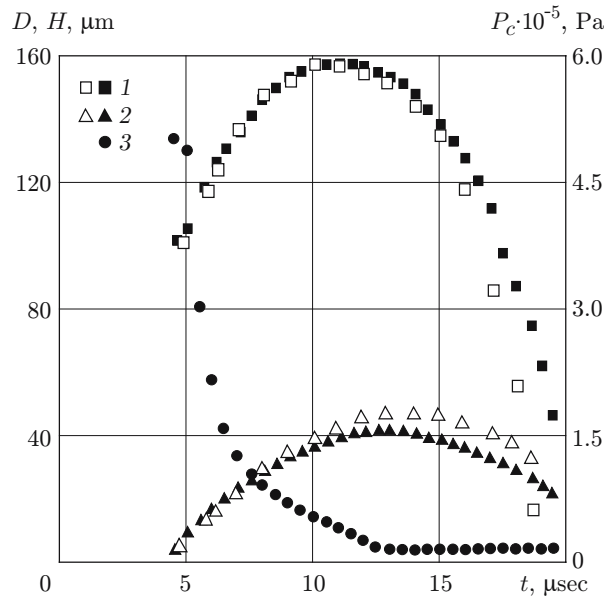


Fig. 2. Changes in the size of the vapor cavity (points 1 and 2) and vapor pressure in the cavity (points 3) in the course of cavity evolution in ethanol ($q = 3.1 \cdot 10^8 \text{ W/m}^2$ and $\tau_h = 4.4 \text{ } \mu\text{sec}$): the open and filled points are the experimental data and calculated results, respectively; curves 1–3 show the cavity size in the radial direction D , the cavity height H , and the vapor pressure P_c , respectively.

with cylindrical symmetry of the heater–cavity system in numerical simulations. The experiments showed that the symmetry of the cavity shape at late stages of its collapse is violated in the case of boiling on square-shaped heaters [14]. The area of the cavity surface increases, which accelerates the collapse.

Figure 3 shows the calculated and experimental duration of cavity evolution $\tau_v = \tau_{cc} - \tau_c$ (time period between cavity formation τ_c and its collapse τ_{cc}) as a function of the heat flux. The influence of the heat flux q on the maximum size of the cavity in the radial direction D_{\max} is illustrated in Fig. 4. It follows from the data presented that the calculated results offer a satisfactory description of the basic features obtained in the experiment. In particular, the results of experiments and numerical simulations show that the maximum size reached by the cavity in the course of evolution and the duration of cavity evolution become smaller as the heat flux increases (see Figs. 3 and 4). The data obtained also suggest that the maximum cavity size is observed for water. In addition, a longer process of cavity growth and collapse is typical of water.

5. Discussion and Conclusions. The calculation results show that the temperature of the liquid near the heater reaches the values corresponding to the beginning of homogeneous boiling faster with increasing heat flux (see Eq. (1) and data described in [14]). In this case, however, the amount of heat stored in the heated layer of the liquid decreases. An increase in the heat flux enhances the rate of bubble generation. The number of bubbles generated increases, but their size reached before their coalescence is smaller. For this reason, the initial volume of the vapor cavity and the internal energy of the vapor are also smaller. Thus, an increase in the heat flux reduces both the internal energy of the vapor in the cavity formed and the amount of heat accumulated in the liquid in the course of heating. As a result, the duration of cavity evolution and the maximum size of the cavity become smaller (see Figs. 3 and 4).

Among the liquids tested, water has the highest temperature of boiling incipience and the maximum values of the thermal conductivity and specific heat, which favors accumulation of a considerable amount of heat in the liquid during its heating. Water is also characterized by the highest pressure of saturated vapors. Despite a high value of the latent heat of evaporation, the above-noted properties of water ensure a significant growth of the cavity. Thus, the greatest values of the cavity size and duration of its evolution were obtained for water, as compared with other examined liquids under identical thermal conditions (see Figs. 3 and 4).

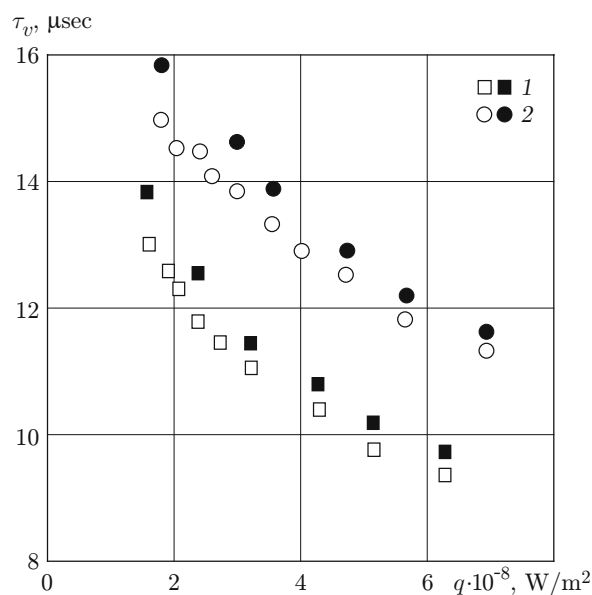


Fig. 3

Fig. 3. Duration of cavity evolution versus the heat flux q : the open and filled points are the experimental and calculated data; the liquids used are toluene (points 1) and ethanol (points 2).

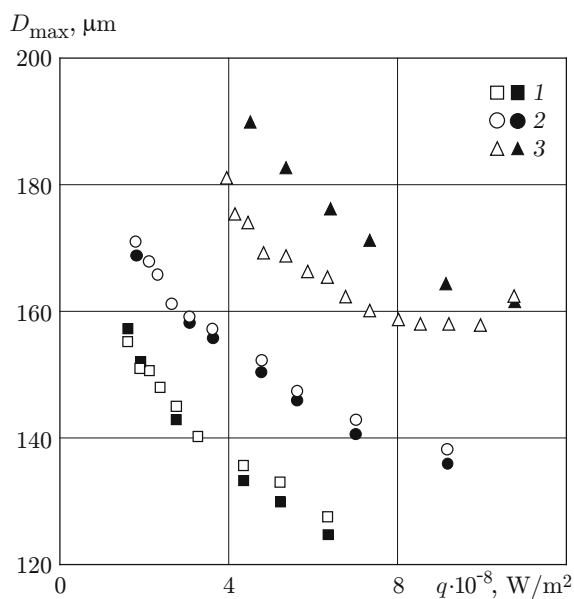


Fig. 4

Fig. 4. Maximum size of the cavity in the radial direction D_{\max} versus the heat flux q : the open and filled points are the experimental and calculated data; the liquids used are toluene (points 1), ethanol (points 2), and water (points 3).

It seems of interest to consider the magnitude and character of variation of the vapor pressure in the cavity in the course of its evolution. As an example, Fig. 2 shows the calculated pressure in the cavity $P_c(t)$ at the stages of its growth and collapse in the case of explosive boiling of ethanol. It should be noted that the initial pressure of the vapor in the cavity formed $P_c(\tau_c)$ is lower than the pressure of saturated vapors at the temperature of boiling incipience of ethanol $P_s \approx 33 \cdot 10^5$ Pa ($T_b = 478$ K) and decreases with increasing cavity size. Because of the inertia of liquid motion and a decrease in the amount of heat stored in the liquid layer around the cavity, the vapor pressure in the cavity becomes lower than the atmospheric value. The cavity ceases to grow and starts to collapse. The velocity of motion of the liquid increases. It is enough time for the heat released during condensation to be removed into the liquid. As a result, the pressure in the cavity remains lower than the atmospheric value until the final stage of the cavity collapse. A similar dependence is also observed for other liquids tested.

Thus, a comparison of numerical simulations with experimental data allows us to conclude that the model proposed offers an adequate description of the basic features of explosive boiling of liquids on film heaters, including the effect of liquid properties and conditions of the thermal action on the process duration and on the size of the vapor structures.

This work was supported by the Russian Foundation for Basic Research (Grant No. 05-08-18064).

REFERENCES

1. V. P. Skripov, *Metastable Liquids* [in Russian], Nauka, Moscow (1972).
2. S. J. D. Van Stralen and R. Cole, *Boiling Phenomena*, Vol. 1, McGraw-Hill, New York (1979).
3. M. Blander and J. L. Katz, "Bubble nucleation in liquids," *AIChE J.*, **21**, No. 5, 833–847 (1975).
4. P. A. Pavlov, "Calculation of heat removal from the heater to the liquid during fluctuation boiling," in: *Nonequilibrium Phase Changes and Thermophysical Properties of Substances* (collected scientific papers) [in Russian], Izd. Ural. Otd. Ross. Akad. Nauk, Ekaterinburg (1996), pp. 57–65.

5. A. Asai, "Three-dimensional calculation of bubble growth and drop ejection in a bubble jet printer," *J. Fluids Eng.*, **114**, 638–641 (1992).
6. L. Lin and A. Pisano, "Thermal bubble powered microactuators," *Microsyst. Technol. J.*, No. 1, 51–58 (1994).
7. H. Yuan and A. Prosperetti, "The pumping effect of growing and collapsing bubbles in a tube," *J. Micromech. Microeng.*, No. 9, 402–413 (1999).
8. M. Volmer, *Kinetics der Phasenbildung*, Steinkopff, Dresden–Leipzig (1939).
9. C. T. Avedisian, "Modeling homogeneous bubble nucleation in liquids," in: *Modelling of Engineering Heat Transfer Phenomena*, Chapter 11, Comput. Mech., London (1998).
10. Y. Iida, K. Okuyama, and K. Sakurai, "Boiling nucleation on a very small film heater subjected to extremely rapid heating," *Int. J. Heat Mass Transfer*, **37**, 2771–2780 (1994).
11. Z. Yin, A. Prosperetti, and J. Kim, "Bubble growth on an impulsively powered microheater," *Int. J. Heat Mass Transfer*, **47**, 1053–1067 (2004).
12. Z. Zhao, S. Glod, and D. Poulikakos, "Pressure and power generation during explosive vaporization on a thin-film microheater," *Int. J. Heat Mass Transfer*, **43**, 281–296 (2000).
13. V. V. Kuznetsov and E. S. Vasserman, "Dynamics of explosive boiling on a mesoporous surface," in: *Dynamics of Continuous Media* (collected scientific papers) [in Russian], No. 117, Inst. Hydrodynamics, Sib. Div., Russian Acad. of Sci. (2001), pp. 25–29.
14. Yu. D. Varlamov, Yu. P. Meshcheryakov, M. R. Predtechenskii, et al., "Specific features of explosive boiling of liquids on a film microheater," *J. Appl. Mech. Tech. Phys.*, **48**, No. 2, 213–220 (2007).
15. S. K. Godunov (ed.), *Numerical Solution of Multidimensional Problems of Gas Dynamics* [in Russian], Nauka, Moscow (1976).